PERGAMON

International Journal of Solids and Structures 36 (1999) 2021–2040

INTERNATIONAL JOURNAL OF SOLIDS and STRUCTURES

Optimum shape and topology design using the boundary element method

K. Tai†, R. T. Fenner*

Mechanical Engineering Department, Imperial College of Science, Technology and Medicine, Exhibition Road, London SW7 2BX, U.K.

Received 23 August 1995; in revised form 11 September 1996

Abstract

A procedure is developed for simultaneous shape and topology design optimization of linear elastic two-dimensional continuum structures. An intuitive approach is presented to treat such topological problems whereby material is eliminated from within the structure (by introducing holes at regions of low stress) through a sequence of shape optimization processes. A mathematical programming technique coupled with the boundary element (BE) method of response and sensitivity analyses enables the optimal positioning of these holes plus optimization of the overall structural shape. The analytical derivative BE formulation is explained together with the use of appropriate design velocity fields, and example problems are solved to demonstrate the optimization procedure.

1. Introduction

Topology design optimization, as part of the wider field of structural optimization, refers to optimal design problems where the performance of a structure or component is optimized through a variation of its topology. In the case of discrete structures such as trusses or frames, topology is described by the number of bars and joints and the order in which the bars are connected to one another. For continuum structures like flat plates or three-dimensional solid bodies, the topological design variables may be the number of holes/cavities or may describe the connectivity of the domain such that the structure is simply- or multiply-connected. In either case, the design variables involved are intrinsically discrete in nature, and topology optimization is essentially a material distribution/arrangement problem.

The study of arrangements is at the core of combinatorics, and discrete optimization can be

* Corresponding author. Tel.: 00 44 171 594 7060; fax: 00 44 171 823 8845; e-mail: r.fenner@ic.ac.uk

† Present address: School of Mechanics and Production Engineering, Nanyang Technological University, Nanyang Avenue, Singapore 639798

0020–7683/99/$ - see front matter
PII: S0020–7683(98)00074–2

considered one form of combinatorial problems and where the solution space may comprise a potentially huge number of feasible permutations/combinations. As differential calculus is applied only to continuous variables and functions, calculus methods may not be used to treat discrete problems which have to be solved by enumerating all or a significant fraction of the solution space. This is the reason why discrete optimization tasks are difficult, as computational order can grow either logarithmically, polynomially or exponentially with the number of discrete choices to be resolved (Parker and Rardin, 1988). The lack of generally reliable and efficient algorithms for such optimization may have discouraged the tackling of problems of practical sizes. Consequently, non-exact procedures based on heuristics and intuition occupy an important place in the field of discrete optimization. These non-exact algorithms can achieve a candidate solution that is feasible, but the solution may or may not be optimal, or may even be arbitrarily far from the true optimum. Nevertheless, discrete decisions are encountered and are inevitable in almost all fields of engineering design, especially with regards to conceptual design. There have been examples of discrete optimization techniques applied to engineering design such as that by Sandgren (1990a, b) where the branch-and-bound method is used to optimize conceptual design decisions like the selection of the material, structural cross-section, and the number of gear teeth to be used in various systems.

Topology design optimization is one area dominated by discrete decisions, and it is the discrete nature of the problem that makes it much more complex and a less well-developed field than shape optimization. However, it is evident that the topology design of a structure, by determining its concept and configuration, has a potentially far greater impact on its performance than does the geometric shape. For generating optimal topologies of truss structures, heuristically- or intuitively-based techniques are usually employed so as to avoid dealing directly with the discrete nature of the problem. Some examples of these are the rule-based methods of Hajela and Sangameshwaran (199) and the ground structure approach by Zhou and Rozvany (1991). For the case of continuum structures, intuitive approaches are also usually adopted. The ability to modify the connectivity of a structure will produce better results in an optimal design procedure compared to the standard shape optimization scheme. Topology design optimization of continuum structures in two-dimensional elastostatics is a problem investigated in this present work, where a procedure is developed to achieve simultaneous shape and topological optimum.

2. Topological optimization technique

For dealing with topology design problems, three conceptually different techniques can be identified from the structural optimization literature. However, the structural analysis procedures used in this area have all been based on the finite element (FE) method. The most well-developed technique is the 'composites/microstructures' approach of Bendsoe and Kikuchi (1988) where the distribution of material is determined through a sizing optimization of material density within the finite elements. This represents the use of composite materials (obtained through perforation) for modelling the structure, with a homogenization method applied to relate the effective modulus to the size and orientation of the hole/perforation in each element. This approach has been described as a relaxed formulation of the optimal shape design problem (Allaire and Kohn, 1993), putting it on a sound mathematical basis. By discretizing the design space, the approach intuitively removes the discrete character of topological optimization and transforms it to a problem with continuous

variables (parameters of the perforations). However, there is still a remaining question of deciding whether an element represents material or void, especially for elements with resulting intermediate densities, and this is the heuristic aspect of the technique necessary to make such yes–no decisions. Different interpretations of the optimal distribution of material in the domain can give rise to topologically different resulting structures.

The second technique for topology optimization is referred to here as the 'element removal' approach as demonstrated by Atrek (1989), Russell and Manoochehri (1989) and Rodriguez and Seireg (1992). In this method, shape and topological changes are effected by removing elements from a structure after an FE analysis. Intuitively-based criteria (usually involving stresses and strains) are used to identify which elements can be eliminated to minimize structural weight subject to maximum stress constraints. The problem definition in this approach is greatly simplified as no mathematical programming optimization techniques are involved and thus there is not even the need to define design variables. However, similar to the composites approach, the resulting structural boundaries usually consist of jagged edges because they are formed by the remaining elements. Pattern recognition and image processing techniques are thus usually necessary to deduce, smoothen and parameterize the final resulting boundaries.

The third technique is referred to here as the 'introduction of hole' approach as performed by Eschenauer and Schumacher (1993) and Eschenauer et al. (1994). An initial shape optimization process is carried out on a structure after which some intuitive criteria are used to locate which regions in the domain are best for introducing cutouts or holes in the design. With the topological change made by adding a hole or cutout, the new modified design is put through another shape optimization process and the whole procedure is repeated until some convergence criteria are satisfied. This approach thus works by performing shape optimization on a sequence of topologically different configurations, and comparing the objective function values among these discrete and distinct alternatives. It is a viable and effective strategy in practice and overcomes the previously mentioned disadvantages of the other two approaches, and it is the technique adopted in this present work. An important difference between this and the previous two approaches is that, in this method, boundary shape parameterization is required as input to the solution procedure. This is because shape optimization problems are treated with design variables defined for the main structural body as well as the inserted holes/cutouts, unlike the composites approach where only a sizing optimization is carried out. Hence a shape optimization scheme is essential to the overall procedure in this approach to be used.

The methodology developed here is similar to that of Eschenauer et al. (1994) except for some important differences. Firstly, the boundary element (BE) method is used instead of the FE method. Being a boundary-oriented technique, the BE method lends itself easily to shape design considerations and is highly accurate for sensitivity analysis. However, as the stress response in the domain is needed for selecting the locations for new holes to be inserted, post-processing of the BE results is necessary to compute stresses at interior points. The second difference is that the holes introduced here are of finite sizes, while those in Eschenauer et al. (1994) are of initial infinitesimal sizes with the assumption that the macroscopic stress field of the main body remains undisturbed while the microscopic stress field will exhibit local stress concentrations in the vicinity of the hole. Thirdly, the holes are to be introduced at points of lowest von Mises equivalent stresses, instead of lowest value of some special characteristic functions derived based on principal stresses. In any case, these hole-positioning criteria are all intuitively-based, and so it has been assumed

here that low von Mises stresses are good indicators of regions where structural material has not been efficiently utilized and can be eliminated. Fourthly, the holes introduced here are of a fixed circular shape and parameterized by design variables of position and size (radius), instead of assuming free-form shapes using shape representation techniques. There is no doubt that allowing arbitrary free-form shape variation will produce results of a stronger optimum; however, using basic circular-shaped holes does keep the procedure simple and reduce the number of design variables to be treated in the optimization process. In addition, the use of basic shape parameterizations only allows holes to be introduced at the domain interior but not at the boundaries, unlike that in Eschenauer et al. (1994) which can also introduce cutouts and notches at the boundaries. Such a capability requires highly sophisticated shape representation techniques such as non-uniform rational B-splines (NURBS) to treat edges with sharp corners. Future work will be carried out in this area to include free-form shape representation techniques in the procedure. The main focus in this present work is to assess the concepts behind the approach and methodology.

3. Topology design methodology

Step 1 *Initial Shape Optimization*: A shape optimization process is carried out on the initial design. The objective function is thus minimized and the optimum shape obtained based on the fixed topological configuration of the initial design.

Step 2 *Response Analysis of Interior Points*: To evaluate the response behaviour of the domain interior, a set of interior points must initially be obtained. This is done by first determining the maximum dimensional extents x_{dim} and y_{dim} of the structural domain in the x- and y-directions, respectively (see the example in Fig. 1). A rectangular grid of points is then established within the

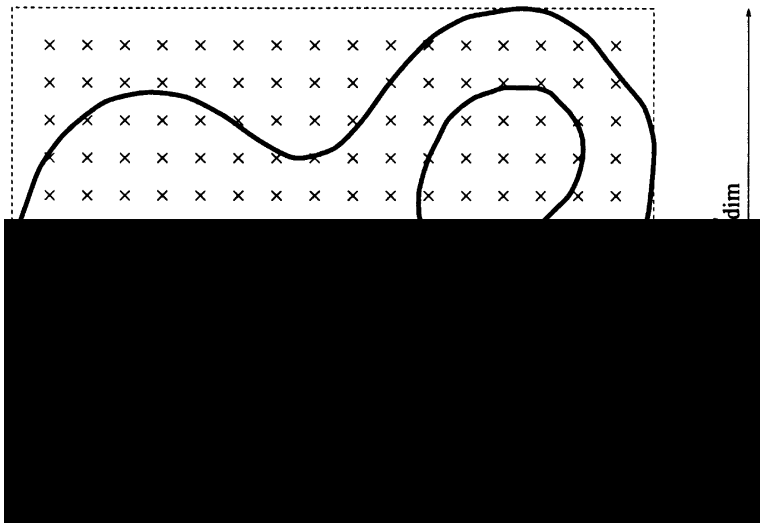

Fig. 1. Grid of points within maximum extent of domain.

maximum extent of the domain. The density of the grid is variable and can be adjusted by changing the numbers of points N_{Gx} and N_{Gy} along the x- and y-directions, respectively.

A procedure is required next to ascertain which of the grid points are interior and which are exterior with respect to the structural domain, so that exterior points can be discarded. Based on a Gauss' theorem formulation, this is done by verifying the angle subtended at each point by segments of the domain boundary through a closed integration round the boundary. Besides checking if the grid point is inside or outside of the domain, the integration process is also used to check that the point is not too near the boundary. Points which are less than a minimum distance $r_{\min}$ from the boundary will also be discarded (even if they are interior) because holes introduced at such points will be too near to the boundary, possibly resulting in boundary interferences or intersections. The minimum distance $r_{\min}$ is determined based on a prescribed fraction $R_{\min}$ of either the maximum extent $x_{\dim}$ or $y_{\dim}$, whichever is the smaller:

$$r_{\min} = R_{\min}[\min(x_{\dim}, y_{\dim})] \tag{1}$$

The appropriate size of fraction $R_{\min}$ is based on heuristics, and a typical value around $R_{\min} = 0.15$ is usually effective.

Once the set of interior points has been obtained, the BE method of response analysis is performed to evaluate the stresses at each point.

Step 3 *Introduction of Hole*: With the results of the interior response available, the interior point with the lowest von Mises equivalent stress is located. The x- and y-coordinates of this point will become the positional coordinates x_{hole} and y_{hole} of the centre of the circular hole to be introduced. The initial radius of this hole r_{hole} is determined based on a prescribed fraction R_{hole} of either the maximum extent $x_{\dim}$ or $y_{\dim}$, whichever is the smaller:

$$r_{\text{hole}} = R_{\text{hole}}[\min(x_{\dim}, y_{\dim})] \tag{2}$$

A typical value of about $R_{\text{hole}} = 0.12$ is usually prescribed. The positional and size parameters (x_{hole}, y_{hole} and r_{hole}) of the new hole introduced will then have to be installed (together with their respective velocity fields) as additional design variables for subsequent shape optimization processes, along with all other existing design variables pertaining to the main structural boundaries and any holes previously introduced. The new hole boundary will also be discretized and added to the existing BE mesh of the structure. It should be noted that the initial hole position is in a small way influenced by the density of grid points used, and the initial hole size is determined by the value of the fraction R_{hole} prescribed. However, the exact size and position of the hole introduced is not critical to the eventual results attained because these parameters are made variable and will be fine-tuned in subsequent shape optimization steps.

As alternatives to the circular hole, holes of other shapes such as slots or ellipses may also be used. These shapes are likely to require parameterization by more design variables than the circle, but as long as the variables are pre-defined together with the necessary velocity field terms, such hole shapes may be used instead. However, circular holes are used here because they are the most generally suitable for altering the structural configuration.

Step 4 *Shape Optimization on Modified Topology*: A shape optimization process is performed to obtain the optimum shape based on the new topological configuration.

Step 5 *Check on Convergence and Termination Criteria*: If the current objective function value is greater than or equal to that of the previous topological configuration, convergence is assumed and the procedure ended by skipping to Step 6. If the number of holes introduced has reached the prescribed maximum allowable number t_{max}, the procedure is to be terminated by skipping to Step 6. If neither the convergence nor termination criterion has been met, the iteration is continued by returning to Step 2.

Step 6 *Termination of Procedure*: The procedure is ended and the optimum design with the lowest objective function value indicates the topological and shape optimal design.

4. Shape design optimization scheme

An effective shape optimization scheme is essential to the overall topology design procedure and this process is reviewed here. The scheme applied is based on a mathematical programming approach coupled with the BE method of response/sensitivity analysis (Tai and Fenner, 1996). There is flexibility with the use of a mathematical programming approach since any design objective can be treated, whereas the optimality criteria approach is usually formulated based on a single objective function such as the elastic compliance. The numerical optimization technique used is the penalty function method with extended interior penalties (Vanderplaats, 1984). Objective and constraint function values/gradients are dependent on the structural response evaluated by the BE method. There is recognition of the advantages for its use in the field shape optimal design, such as the more accurate boundary stress calculations compared to the FE method (Mota Soares and Choi, 1986). Furthermore, as the topology design procedure modifies the variable (external) boundary shape of the structure plus the positions and sizes of the circular holes introduced, the BE method is very suitable since no discretization is needed inside the domain. This is because the BE mesh of the hole is 'free-floating' within the main body, and so variations of the hole position, size and shape do not disturb the discretization around the rest of the structure. This reduces the computation required with regards to velocity field terms and remeshing of the whole structure, making the BE method very useful for such optimal feature positioning problems.

The BE formulation for linear elasticity (Becker, 1992) directly treats the response quantities of displacement u_j and traction t_j based on the following analytical boundary integral equation (BIE)

$$C_{ij}(P)u_j(P)+\int_\Gamma T_{ij}(P,Q)u_j(Q)\,\mathrm{d}\Gamma(Q)=\int_\Gamma U_{ij}(P,Q)t_j(Q)\,\mathrm{d}\Gamma(Q) \tag{3}$$

where P and Q are, respectively, the boundary load and field points, Γ is the field boundary, U_{ij} and T_{ij} are, respectively, the displacement and traction kernels (Kelvin's solution), and C_{ij} is a Cauchy principal limiting value dependent on the boundary geometry at load point (but can be readily determined through considerations of rigid-body motion). Tensor notation is used to represent spatial dimensionality where appropriate, with the summation convention implied for repeated indices. The kernel functions in the BIE are evaluated as follows

$$U_{ij}(P,Q)=\frac{1}{8\pi\mu(1-\nu)}\left[(3-4\nu)\ln\left(\frac{1}{r}\right)\delta_{ij}+\frac{\partial r}{\partial x_i}\frac{\partial r}{\partial x_j}\right] \tag{4}$$

$$T_{ij}(P,Q)=\frac{-1}{4\pi(1-\nu)}\left(\frac{1}{r}\right)\left\{\frac{\partial r}{\partial n}\left[(1-2\nu)\delta_{ij}+2\frac{\partial r}{\partial x_i}\frac{\partial r}{\partial x_j}\right]+(1-2\nu)\left(\frac{\partial r}{\partial x_j}n_i-\frac{\partial r}{\partial x_i}n_j\right)\right\} \tag{5}$$

where

$$\frac{\partial r}{\partial n}=\frac{\partial r}{\partial x_i}\frac{\partial x_i}{\partial n} \tag{6}$$

$$\frac{\partial r}{\partial x_i}=\frac{x_i-\zeta_i}{r} \tag{7}$$

$$\frac{\partial x_i}{\partial n}=n_i \tag{8}$$

$$r=r(P,Q)=(x_ix_i-2x_i\zeta_i+\zeta_i\zeta_i)^{1/2} \tag{9}$$

where δ_{ij} is the Kronecker delta, r is the distance between the load and field points, ζ_i and x_i are, respectively, the coordinate positions of the load and field points, n_i is the unit outward normal at the field point, μ is the shear modulus and ν is the Poisson's ratio.

The numerical implementation of the BIE (3) is performed by discretization using isoparametric quadratic boundary elements, followed by a systematic point collation procedure to assemble the set of linear algebraic equations based on taking each boundary node in turn as the load point. After solving the equation set for the unknown displacements/tractions, boundary tangential strains are evaluated so that boundary stresses can be determined through the stress–strain relations. As the topology design procedure requires stress values at the domain interior, these stresses σ_{ij} at each interior point are obtained by treating that point as the load point p in the Somigliana's identity for stresses

$$\sigma_{ij}(p)+\int_\Gamma S_{kij}(p,Q)u_k(Q)\,\mathrm{d}\Gamma(Q)=\int_\Gamma D_{kij}(p,Q)t_k(Q)\,\mathrm{d}\Gamma(Q) \tag{10}$$

where the third-order tensors S_{kij} and D_{kij} are defined as follows

$$\begin{aligned}S_{kij}(p,Q)=&\frac{\mu}{2\pi(1-\nu)}\left(\frac{1}{r^2}\right)\left\{n_i\left[2\nu\frac{\partial r}{\partial x_i}\frac{\partial r}{\partial x_k}+(1-2\nu)\delta_{jk}\right]+n_j\left[2\nu\frac{\partial r}{\partial x_k}\frac{\partial r}{\partial x_i}+(1-2\nu)\delta_{ki}\right]\right.\\&\left.+n_k\left[2(1-2\nu)\frac{\partial r}{\partial x_i}\frac{\partial r}{\partial x_j}-(1-4\nu)\delta_{ij}\right]\right\}+\frac{\mu}{\pi(1-\nu)}\left(\frac{1}{r^2}\right)\frac{\partial r}{\partial n}\left[(1-2\nu)\frac{\partial r}{\partial x_k}\delta_{ij}\right.\\&\left.+\nu\left(\frac{\partial r}{\partial x_i}\delta_{jk}+\frac{\partial r}{\partial x_j}\delta_{ki}\right)-4\frac{\partial r}{\partial x_i}\frac{\partial r}{\partial x_j}\frac{\partial r}{\partial x_k}\right]\end{aligned} \tag{11}$$

$$D_{kij}(p,Q)=\frac{1}{4\pi(1-\nu)}\left(\frac{1}{r}\right)\left[(1-2\nu)\left(\frac{\partial r}{\partial x_i}\delta_{jk}+\frac{\partial r}{\partial x_j}\delta_{ki}-\frac{\partial r}{\partial x_k}\delta_{ij}\right)+2\frac{\partial r}{\partial x_i}\frac{\partial r}{\partial x_j}\frac{\partial r}{\partial x_k}\right] \tag{12}$$

Sensitivity analysis with the BE method is carried out by an implicit analytical differentiation of the BIE (3). By differentiating with respect to an entirely arbitrary geometric variable, any structural

shape design variation can be handled. Whole boundary segments can be made variable, in addition to localized shape changes. Hence problems of the optimum positioning of features can also be solved, as required in the topology design procedure where the positions of holes introduced are optimized simultaneously with the overall structural shape. The derivative BIE is thus given by

$$\begin{aligned} &C'_{ij}(P)u_j(P)+C_{ij}(P)u'_j(P)\\ &+\int_\Gamma [T'_{ij}(P,Q)u_j(Q)+T_{ij}(P,Q)u'_j(Q)]\,\mathrm{d}\Gamma(Q)+\int_\Gamma T_{ij}(P,Q)u_j(Q)[\,\mathrm{d}\Gamma(Q)]'\\ &=\int_\Gamma [U'_{ij}(P,Q)t_j(Q)+U_{ij}(P,Q)t'_j(Q)]\,\mathrm{d}\Gamma(Q)+\int_\Gamma U_{ij}(P,Q)t_j(Q)[\,\mathrm{d}\Gamma(Q)]' \end{aligned} \tag{13}$$

where the primed quantities denote the derivative with respect to the design variable. The displacement and traction kernels are differentiated as follows

$$U'_{ij}(P,Q)=\frac{1}{8\pi\mu(1-\nu)}\left[(3-4\nu)\left(\ln\frac{1}{r}\right)'\delta_{ij}+\left(\frac{\partial r}{\partial x_i}\right)'\frac{\partial r}{\partial x_j}+\frac{\partial r}{\partial x_i}\left(\frac{\partial r}{\partial x_j}\right)'\right] \tag{14}$$

$$\begin{aligned} T'_{ij}(P,Q)=&\frac{-1}{4\pi(1-\nu)}\left(\frac{1}{r}\right)'\left\{\frac{\partial r}{\partial n}\left[(1-2\nu)\delta_{ij}+2\frac{\partial r}{\partial x_i}\frac{\partial r}{\partial x_j}\right]+(1-2\nu)\left(\frac{\partial r}{\partial x_j}n_i-\frac{\partial r}{\partial x_i}n_j\right)\right\}\\ &-\frac{1}{4\pi(1-\nu)}\left(\frac{1}{r}\right)\left\{\left(\frac{\partial r}{\partial n}\right)'\left[(1-2\nu)\delta_{ij}+2\frac{\partial r}{\partial x_i}\frac{\partial r}{\partial x_j}\right]+2\frac{\partial r}{\partial n}\left[\left(\frac{\partial r}{\partial x_i}\right)'\frac{\partial r}{\partial x_j}+\frac{\partial r}{\partial x_i}\left(\frac{\partial r}{\partial x_j}\right)'\right]\right.\\ &\left.+(1-2\nu)\left[\left(\frac{\partial r}{\partial x_j}\right)'n_i-\left(\frac{\partial r}{\partial x_i}\right)'n_j+\frac{\partial r}{\partial x_j}n'_i-\frac{\partial r}{\partial x_i}n'_j\right]\right\} \end{aligned} \tag{15}$$

where

$$\left(\frac{\partial r}{\partial n}\right)'=\left(\frac{\partial r}{\partial x_i}\right)'\frac{\partial x_i}{\partial n}+\frac{\partial r}{\partial x_i}\left(\frac{\partial x_i}{\partial n}\right)' \tag{16}$$

$$\left(\frac{\partial r}{\partial x_i}\right)'=\left(\frac{1}{r}\right)'(x_i-\zeta_i)+\frac{x'_i-\zeta'_i}{r} \tag{17}$$

$$\left(\frac{\partial x_i}{\partial n}\right)'=n'_i \tag{18}$$

$$r'=\frac{1}{r}(x_ix'_i-x'_i\zeta_i-x_i\zeta'_i+\zeta_i\zeta'_i) \tag{19}$$

It can be noted that all the derivatives expressed so far are ultimately dependent on the terms ζ'_i and x'_i which are derivatives of boundary point positions. These represent the design velocity field that indicate the geometric sensitivity of the point with respect to the design variable. By an appropriate definition of velocity terms, and design variable or shape control parameter can be

treated. Entire segments of the boundary, and not just a single material point alone, can therefore be governed by one single geometric variable. Basic geometric parameters, including the radial size of circular holes and translational position of boundary segments, are used here. The following list shows how velocity fields are defined for the various design variables v:

(a) v is the translational position of a boundary segment:

$$x_i = v + \bar{x}_i, \tag{20}$$

$\bar{x}_i$ = fixed relative position of material point from a reference point of the boundary segment

$$x_i' = 1 \tag{21}$$

(b) v is the radius of a circular arc boundary segment:

$$x_i = v\bar{x}_i, \quad \bar{x}_i = \text{fixed direction cosine (of normal to boundary) at material point} \tag{22}$$

$$x_i' = \bar{x}_i \tag{23}$$

(c) v is the position of one end point of a straight line segment:

$$x_i = v + \rho(\bar{v} - v), \quad \bar{v} = \text{fixed position of the opposite end point of line segment} \tag{24}$$

$$x_i' = 1 - \rho, \tag{25}$$

ρ = fixed proportional (intrinsic) distance of material point along segment from v

With the BE sensitivity analysis formulation, velocity terms are only required at boundary nodal points since only the boundary is discretized and treated directly. Hence there is no need for computation with regards to velocity field in the domain.

5. Numerical results

In this section, a total of three topology and shape optimal design problems are demonstrated on two different structures. The structural dimensions, material properties and other quantities are indicated without units as they can assume any compatible system of units. At the start of each problem a shape optimization process is carried out on the initial design, followed subsequently by one shape optimization procedure after each change of topology (upon introduction of a hole). The topological configuration of the initial design is referred to as configuration 0, while that of the design after the first change of topology (addition of the first hole) is configuration 1, and so on. The shape optimum designs obtained for the various configurations are illustrated by a sequence of two-dimensional stress contour plots of the structural domain.

5.1. *Minimization of compliance and weight of a cantilever beam*

This problem involves a cantilever beam with a uniformly distributed load at a small portion of its underside near the free end (see Fig. 2). There are three design variables which affect the geometry of the beam. The first is v_1 which is the height of the beam at the fixed end. The other two variables are v_2 and v_3 which are the angles controlling the orientations and lengths of the free end and top edge of the beam. The bottom edge is of a constant length and is horizontal. A similar

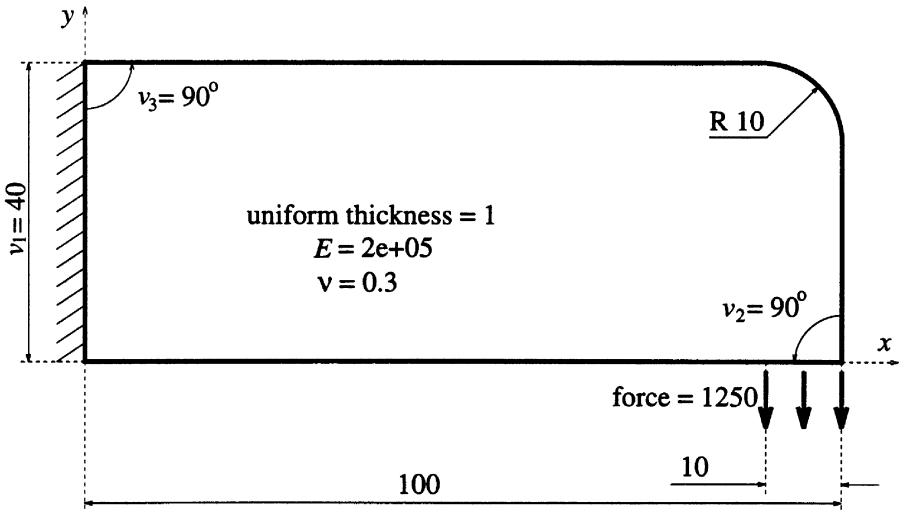

Fig. 2. Cantilever beam under load near free end.

cantilever beam problem has also been solved by Eschenauer et al. (1994) using the FE method and with more complex shape design variables, and minimizing the elastic compliance subject to constraints on the structural volume. In this present example, however, the compliance is also minimized subject to constraints on the maximum material volume but with additional constraints on the maximum allowable von Mises equivalent stresses. The inequality constraints imposed on this problem therefore involve an upper limit $A_{\text{limit}}^{\text{upper}} = 4500$ on the area of the structure, plus an upper limit $\sigma_{\text{limit}}^{\text{upper}} = 250$ on the equivalent stresses around the structure. Assuming a uniform thickness for the beam, the area is a measure of the volume of material in the structure.

The structural area and its derivatives are evaluated analytically based on the design variables and other dimensions of the beam. The elastic compliance objective and stress constraint functions and their derivatives are computed numerically through plane stress BE analyses. The compliance is evaluated as proportional to the strain energy II of the structure:

$$\Pi = \frac{1}{2}\int_{\Gamma} t_j u_j \, \mathrm{d}\Gamma \tag{26}$$

The results of the overall shape and topology design procedure are illustrated in the objective function iteration history plot (Fig. 3) showing how the compliance has been reduced. The iteration plot is not continuous but is broken into four parts, one for each topological configuration (configurations 0, 1, 2 and 3). At the initial design point (iteration number 0), the area constraint is satisfied but the stress constraints are violated. Topological configuration 0 is that of the initial design, and the optimum shape obtained at the end of the optimization procedure performed on this configuration is given by iteration number 14. A hole is then introduced to form the next configuration (configuration 1) and the whole process is then repeated in an iterative manner. As can be seen from the first design point of configuration 1 (at iteration number 15), the addition of a hole has caused the violation of stress constraints (and this also tends to be true for the rest of

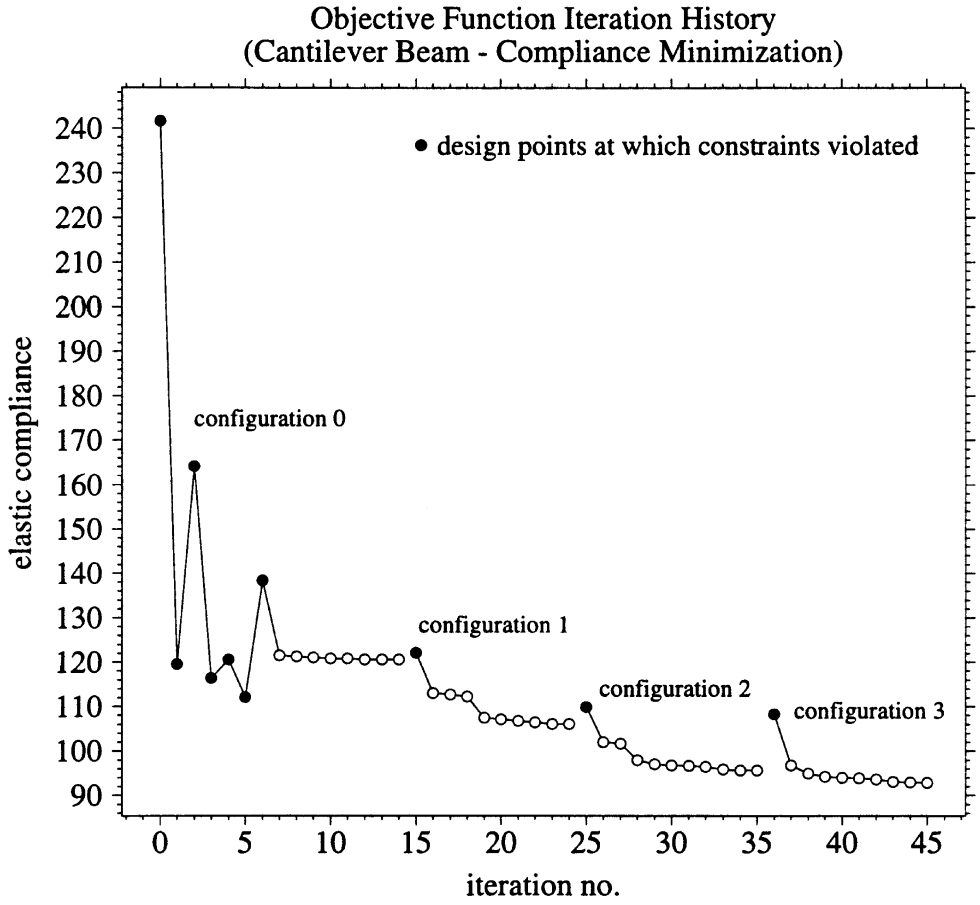

Fig. 3. Plot of objective function iteration history (cantilever beam—compliance minimization).

the configurations 2 and 3). The overall design procedure has been terminated at the end of configuration 3 because the prescribed maximum allowable number of holes to be introduced is $t_{\max} = 3$. It is uncertain whether the addition of one more hole will make a further significant reduction of the objective function but, in any case, with only a small improvement in the optimum compliance value from configuration 2 to 3, it is unlikely that further addition of holes will be effective. From the shape optimum at the end of initial configuration 0 to the shape and topological optimum at the end of configuration 3, the compliance of the structure has been reduced by 23%. This shows that, as expected, the performance of a structure can be further improved and a stronger optimum should be attainable when the topology (and not just the shape) of the structure is allowed to vary. The von Mises equivalent stress contour plots of the optimum structural shapes resulting at the end of each topological configuration is shown in Fig. 4. The circle in dashed lines within the contour plot of any particular configuration shows the initial position and size of the hole to be introduced at the beginning of the following configuration. The optimum shape (from configuration 0) can be compared to the optimum shape and topology (from configuration 3) in

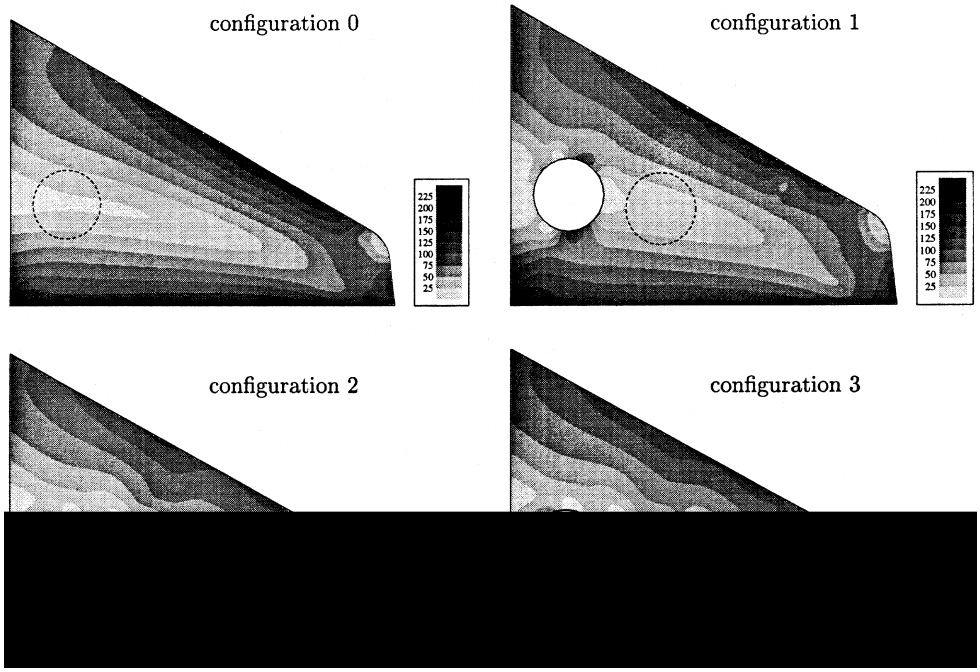

Fig. 4. Equivalent stress contour plots for optimum shapes of different topological configurations (cantilever beam—compliance minimization).

Fig. 5. The results obtained from the procedure here may not be directly comparable to those from Eschenauer et al. (1994) because of the use of free-form shape functions and the introduction of cutouts at boundaries by the latter. However, the final overall shapes and the regions where material has been removed are quite similar between the two.

A second and different optimal design problem is next formulated based on the same cantilever beam structure. This is a weight minimization problem where the structural weight is minimized subject to constraints on the maximum von Mises equivalent stresses. Assuming a uniform mass density and beam thickness, minimizing the weight is equivalent to minimizing the area of the structure. All the other conditions and parameters are the same as in the previous compliance minimization problem, except that a value of $v_1 = 70$ is used for the initial height of the beam instead of $v_1 = 40$ as in the former case.

The results of the overall procedure are shown in the objective function iteration history plot (Fig. 6) indicating how the structural area has been reduced. It can be seen that the optimum objective function value at the end of configuration 3 is worse than that of configuration 2, signifying that convergence has been attained in the solution process and the optimum design is given by that in configuration 2 (with only two holes introduced). The addition of the third hole has worsened the design and increased the objective function (increased the material volume needed to maintain the stresses within the allowable limit). With this hole already added, one way to improve on the objective function is to have the hole eliminated in some way. That is probably

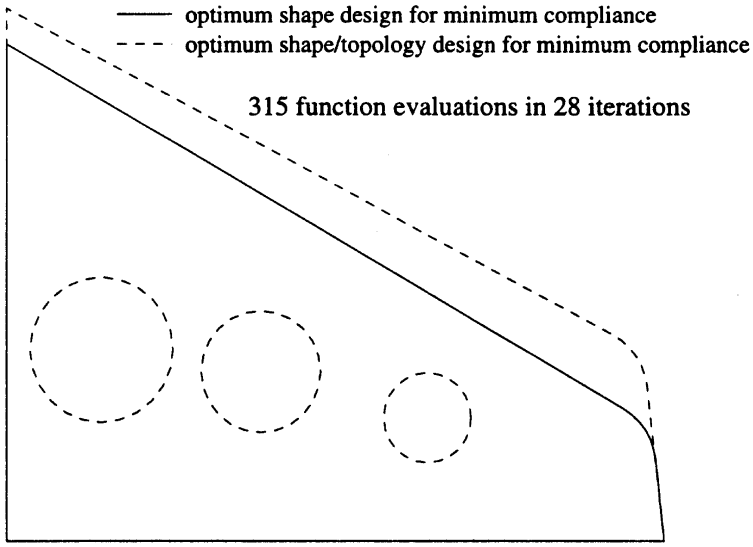

Fig. 5. Optimum shape and optimum shape/topology designs (cantilever beam—compliance minimization).

the reason why, in the shape optimization process of configuration 3, the size of the third hole (plus that of the neighbouring second hole) has been significantly reduced. This can be seen from the stress contour plots of the optimum shapes for the various topological configurations (Fig. 7). From the optimum shape (of configuration 0) to the optimum shape and topology (of configuration 2), the structural area has been reduced by about 21%, and these two designs are compared in Fig. 8. It can also be seen that the optimum shapes obtained in this problem are significantly different from those in the preceding minimum compliance problem.

5.2. *Weight minimization of a connection bracket*

This problem represents a typical connection bracket or plate used to secure two frame members or beams (inclined at certain angles) to a vertical support (see Fig. 9). The bracket is loaded through the bolted joint with the frame members while being fully fixed to the support by, for example, welding. The loads acting at the four bolt holes are in the same directions at their corresponding frame members. The arrangement of the bolt group is fixed relative to the support, and only the outer shape (and topology) of the connection bracket is variable. The straight-edged four-sided concept of the bracket is retained, but the positions of the four corners are variable. Hence design variables v_1, v_2, v_5 and v_6 define the x- and y-coordinates of the two free corners while v_3 and v_4 are the y-coordinates of the two corners at the fixed (supported) vertical edge.

The objective is to minimize the weight subject to constraints on the maximum von Mises equivalent stresses around the bracket. Assuming a uniform mass density and plate thickness, minimizing the weight is equivalent to minimizing the area and hence the objective function is

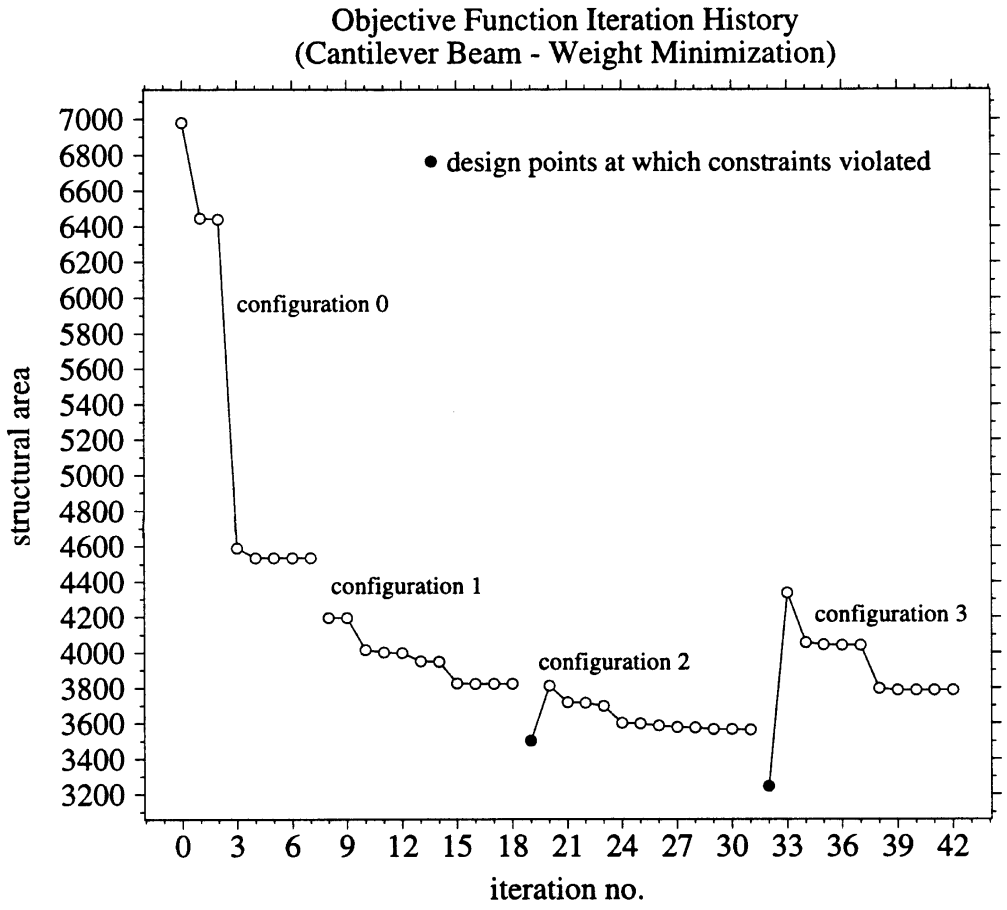

Fig. 6. Plot of objective function iteration history (cantilever beam—weight minimization).

simply the area of the bracket (which is evaluated analytically). The optimization procedure is carried out with the maximum allowable equivalent stress as $\sigma_{\underset{\text{limit}}{\text{upper}}} = 250$.

Results of the overall design procedure are shown in the objective function iteration history (Fig. 10). The procedure has been terminated at the end of configuration 3 as the prescribed maximum number of holes to be introduced is $t_{\max} = 3$. The equivalent stress contour plot of the optimum shape for each topological configuration is shown in Fig. 11, where the circles in dashed lines show where the holes are introduced. There is a $17\frac{1}{2}\%$ reduction in area from the optimum shape at the end of initial configuration 0 to the optimum shape and topology design at the end of configuration 3, and these two designs are compared in Fig. 12.

6. Conclusion

Some of the basic concepts regarding topology design optimization of linear elastic continua have been discussed in this paper. The discrete nature of such problems is recognized and an

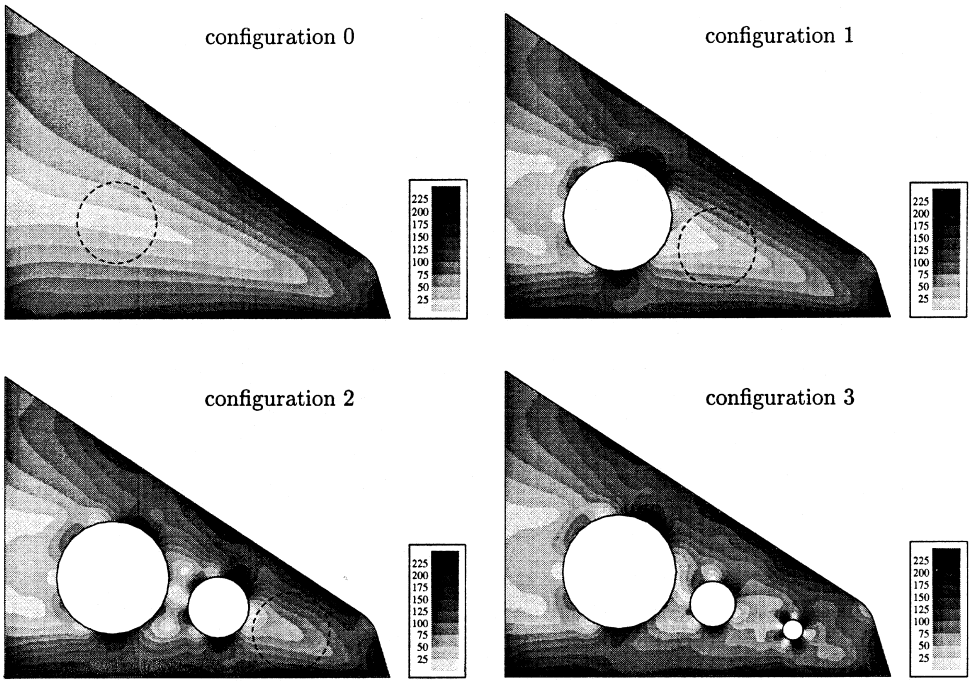

Fig. 7. Equivalent stress contour plots for optimum shapes of different topological configurations (cantilever beam—weight minimization).

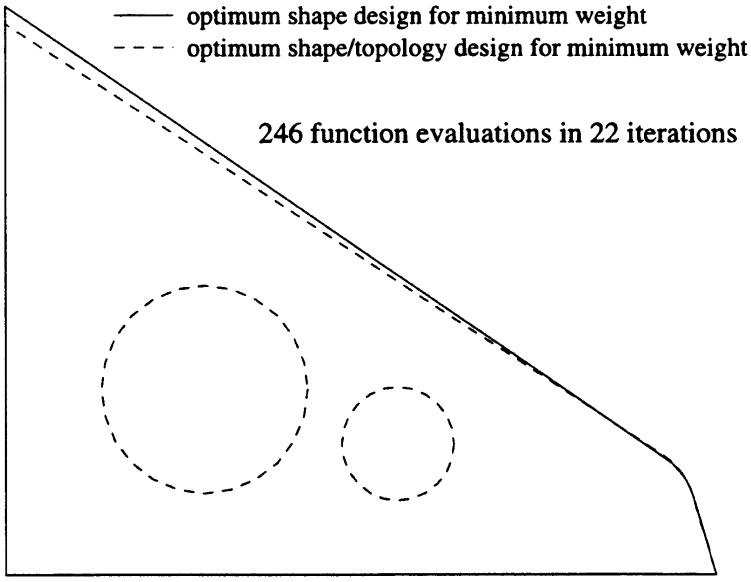

Fig. 8. Optimum shape and optimum shape/topology designs (cantilever beam—weight minimization).

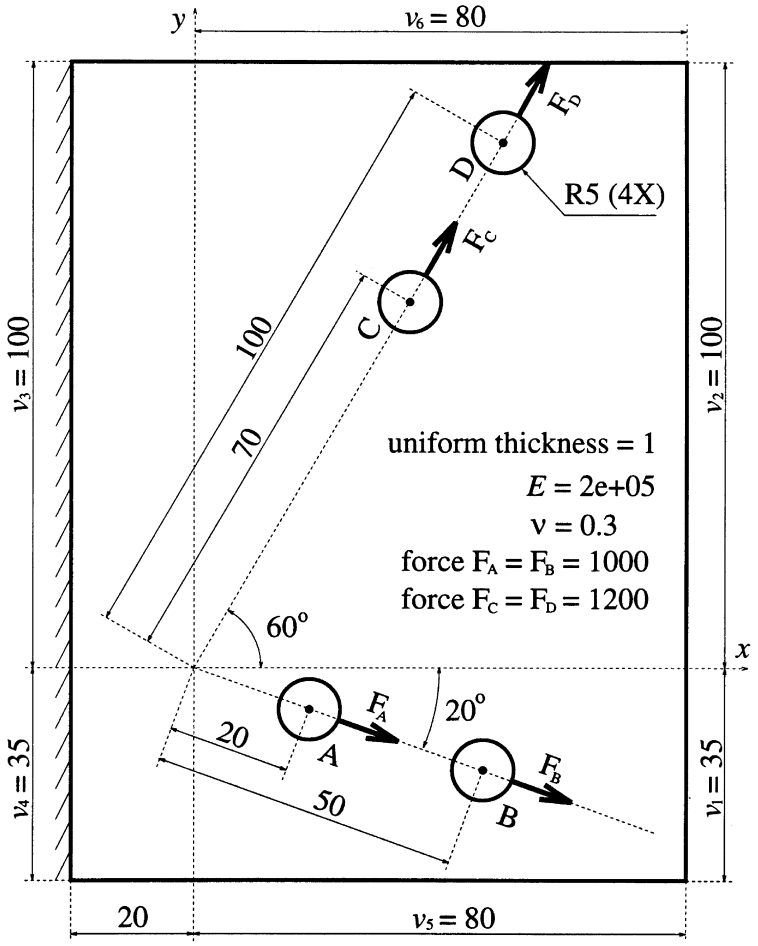

Fig. 9. Connection bracket loaded through bolted joint.

intuitive approach is adopted to optimize structural topology because, with the present state of knowledge in this field, such discrete optimization problems have not been solved other than by a heuristic/intuitive approach.

Topological changes are made by the removal of material from within a structure (by the introduction of holes). Therefore the overall strategy used here is actually to solve a sequence of shape optimization problems each belonging to a different topology configuration (as the number of holes increases). There is uncertainty if or when the optimum topology has been reached since there are no optimality conditions to indicate the optimum point for discrete optimization problems (other than checking the infinite number of all feasible solutions). Therefore holes are added up to the point where the objective function start to worsen or up to a prescribed maximum number of holes, and the best result is taken as the optimum topology and shape. It is noted that the idea

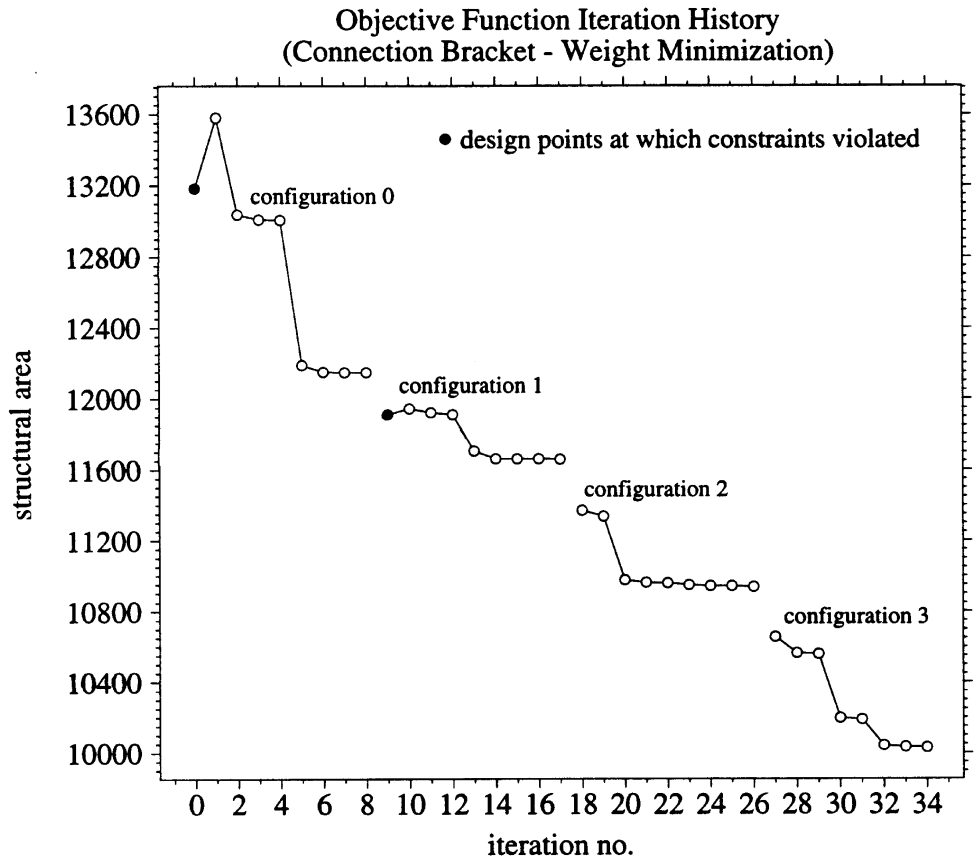

Fig. 10. Plot of objective function iteration history (connection bracket).

of introducing holes and the criteria for deciding their initial positions are all based on intuitive concepts with no formal mathematical foundation provided. After a hole is introduced, its position and size together with the shape parameters of the rest of the structure (and any holes previously introduced) are then varied to reach an optimum shape. The initial position/size of a hole is deemed not to be a critical factor in the solution process except for the possibility that the results obtained may be a local optimum. This is just a limitation of conventional numerical optimization methods which cannot guarantee a global optimum result.

Unlike previous work in this area where the FE method is sued, a BE formulation is applied here with some of its advantages highlighted. With encouraging results demonstrated by the example problems solved, work is ongoing to extend the methodology by incorporating more comprehensive shape variations using free-form shape parameterization techniques.

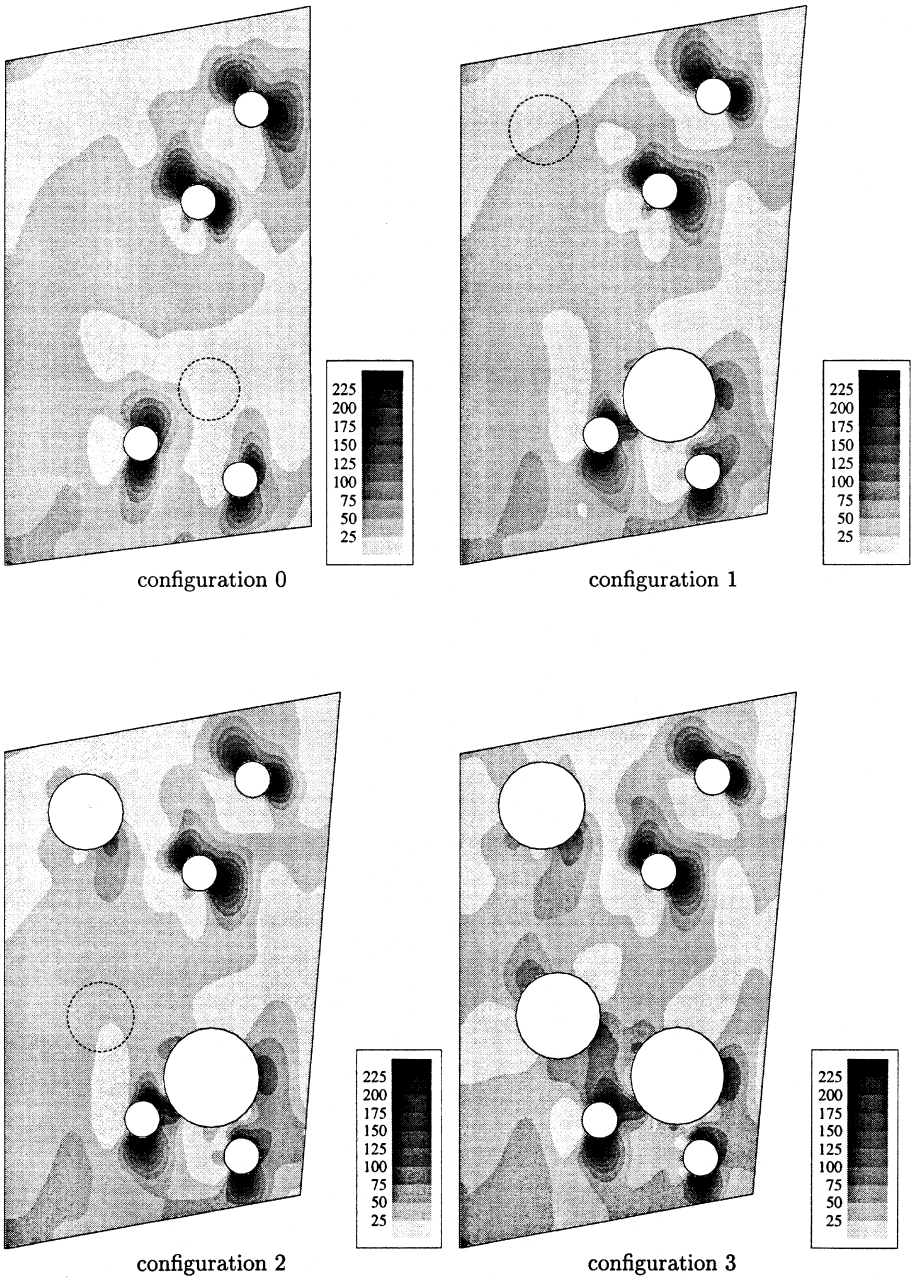

Fig. 11. Equivalent stress contour plots for optimum shapes of different topological configurations (connecting bracket).

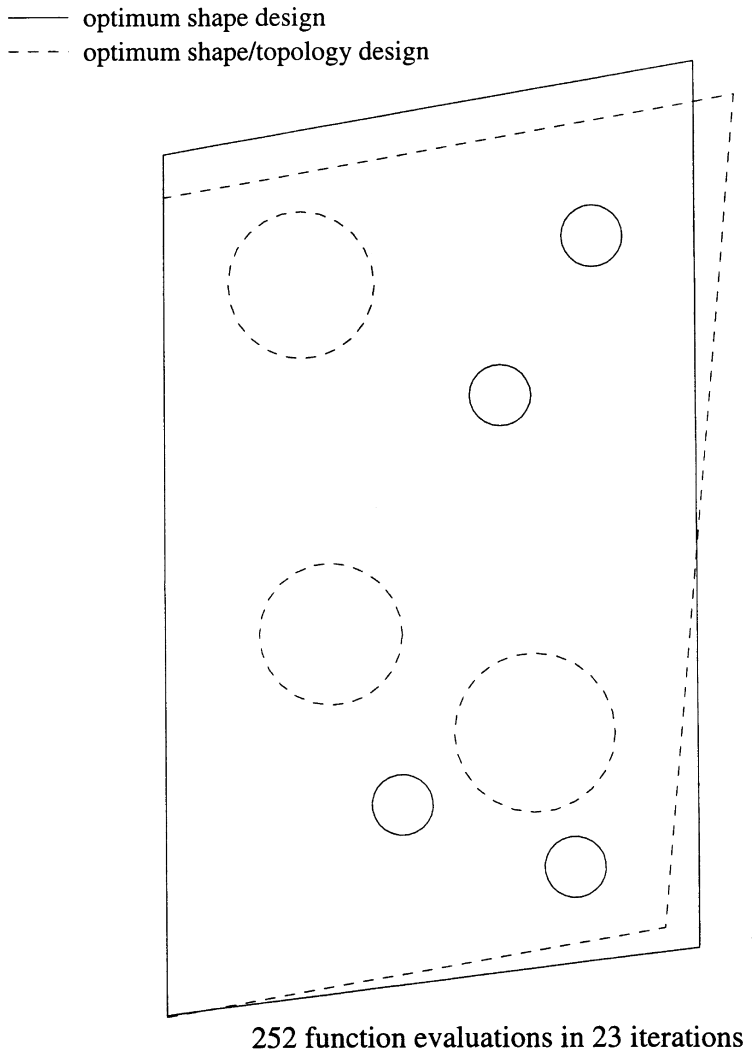

Fig. 12. Optimum shape and optimum shape/topology designs (connection bracket).

References

Allaire, G, Kohn, R.V., 1993. Optimal design for minimum weight and compliance in plane stress using extremal microstructures. Euro. J. Mech., A/Solids 12, 839–878.

Atrek, E., 1989. SHAPE : a program for shape optimization of continuum structures. In : Brebbia, C.A., Hernandez, S. (Eds.), Computer Aided Optimum Design of Structures : Applications. Computational Mechanics Publications, Southampton, pp. 135–144.

Becker, A.A., 1992. The Boundary Element Method in Engineering. McGraw-Hill, London.

Bendsoe, M.P., Kikuchi, N., 1988. Generating optimal topologies in structural design using a homogenization method. Comput. Meth. Appl. Mech. Engng 71, 197–224.

Eschenauer, H.A., Schumacher, A., 1993. Bubble-method : a special strategy for finding best possible initial designs. In :

Gilmore, B.J., Hoeltzel, D.A., Azarm, S., Eschenauer, H.A. (Eds.), Advances in Design Automation, 1993, Vol. 2. ASME, New York, pp. 437–443.

Eschenauer, H.A., Kobelev, V.V., Schumacher, A., 1994. Bubble method for topology and shape optimization and structures. Struct. Opt. 8, 42–51.

Hajela, P., Sangameshwaran, N., 1990. A coupled algorithmic and heuristic approach for optimal structural topology generation. Comput. Struct. 36, 971–977.

Mota Soares, C.A., Choi, K.K., 1986. Boundary elements in shape optimal design of structures. In: Bennett, J.A., Botkin, M.E. (Eds.), The Optimum Shape—Automated Structural Design. Plenum Publishing, New York, pp. 199–231.

Parker, R.G., Rardin, R.L., 1988. Discrete Optimization. Academic Press, London.

Rodriguez, J., Seireg, A.A., 1992. Algorithmic rule-based methodology for shape synthesis: 2-D cases. Comput. Aid. Des. 24, 411–424.

Russell, D.M., Manoochehri, S.P., 1989. A two-dimensional rule-based shape synthesis method. In: Ravani, B. (Ed.), Advances in Design Automation—1989—vol. 2 Design Optimization. ASME, New York, pp. 217–223.

Sandgren, E., 1990a. Nonlinear integer and discrete programming for topological decision making in engineering design. J. Mech. Des. 112, 118–122.

Sandgren, E., 1990b. Nonlinear integer and discrete programming in mechanical design optimization. J. Mech. Des. 112, 223–229.

Tai, K., Fenner, R.T., 1996. Optimum shape design and positioning of features using the boundary integral equation method. Int. J. Numer. Methods Eng. 39, 1985–2003.

Vanderplaats, G.N., 1984. Numerical Optimization Techniques for Engineering Design with Applications. McGraw-Hill, New York.

Zhou, M., Rozvany, G.I.N., 1991. The COC Algorithm, Part II: Topological, geometrical and generalized shape optimization. Comput. Meth. Appl. Mech. Engng 89, 309–336.